

RSC Advances



This is an *Accepted Manuscript*, which has been through the Royal Society of Chemistry peer review process and has been accepted for publication.

Accepted Manuscripts are published online shortly after acceptance, before technical editing, formatting and proof reading. Using this free service, authors can make their results available to the community, in citable form, before we publish the edited article. This *Accepted Manuscript* will be replaced by the edited, formatted and paginated article as soon as this is available.

You can find more information about *Accepted Manuscripts* in the [Information for Authors](#).

Please note that technical editing may introduce minor changes to the text and/or graphics, which may alter content. The journal's standard [Terms & Conditions](#) and the [Ethical guidelines](#) still apply. In no event shall the Royal Society of Chemistry be held responsible for any errors or omissions in this *Accepted Manuscript* or any consequences arising from the use of any information it contains.

Cite this: DOI: 10.1039/c0xx00000x

www.rsc.org/xxxxxx

ARTICLE TYPE

Metal Complexes Bearing 2-(Imidazol-2-yl)phenol Ligands: Synthesis, Characterization and Catalytic Performance in the Fixation of Carbon Dioxide with Epoxides

Jing Peng^{a,b}, Hai-Jian Yang^{*,b}, Zidong Wei^a, Cun-Yue Guo^{*,c}

⁵ Received (in XXX, XXX) Xth XXXXXXXXX 2015, Accepted Xth XXXXXXXXX 2015
DOI: 10.1039/b000000x

A series of metal complexes bearing 2-(imidazol-2-yl)phenol ligands (Zn, Cu, Ni, Co, Pb) were synthesized and their structures were characterized by IR, NMR, elemental analysis and X-ray. The catalytical activities of all complexes for the coupling reaction of CO₂ and epoxide were then detected. The activity influence factors, such as temperature, time, pressure, substituents of ligands and metal centre, were systematically investigated. All these complexes were efficient to catalyze the coupling of CO₂ and epoxide to generate cyclic carbonate in perfect yields (>90%) and selectivities (>99%) under optimized conditions of (2 MPa, 5 h, 110 °C) without any organic solvents. A 99.7% yield and >99% selectivity for propylene carbonate (PC) were obtained with C₇/n-Bu₄NI as catalyst system under the optimized conditions. The catalysts were also proved to be applicable to other terminal epoxides. It is worthy noted that the Pb(II) complex was firstly used to catalyze the coupling reaction of epoxides with carbon dioxide. Moreover, these metal catalysts were recyclable with only minor losses in catalytic activity after simple separation. Finally, a plausible mechanism was given.

1. Introduction

As an alternative, sustainable feedstock for the chemical industry, the conversion of CO₂ into useful chemicals has become a public concern due to the global warming and severe energy crisis.¹⁻⁴ The coupling reaction of CO₂ with epoxides to produce either polycarbonates⁵⁻⁷ or cyclic carbonates⁸⁻¹¹ is considered to be one of the promising routes for CO₂ utilization. The cyclic carbonates, especially five-membered cyclic carbonates, are one kind of CO₂ fixation products and widely used as monomer for polymer synthesis, aprotic solvents, electrolytes for lithium-ion batteries, and as intermediates in the manufacture of fine chemicals.¹²⁻¹⁴ This approach is 100% atom economical and benefits from eliminating phosgene as a reagent.

Recently, numerous homogeneous and heterogeneous catalysts have been used for the synthesis of the cyclic carbonates. Homogeneous catalysts include salen, porphyrin, phthalocyanine and other complexes of the main group and transition metals,¹⁵⁻¹⁸ quaternary ammonium salts,¹⁹ ionic liquids,^{20,21} polyoxometalates²², Lewis acids or bases²³⁻²⁵ and so on. Some heterogeneous catalysts²⁶ also have been explored for the cycloaddition of CO₂ to epoxides, such as metal oxides,²⁷ immobilized complexes or ionic liquids,²⁸⁻³³ titanosilicates,³⁴ and zeolites.³⁵ There are also few examples of the use of the metal-organic frameworks (MOFs).³⁶⁻³⁸ Among these catalyst systems, metal complexes have been of significant interest due to their easy synthesis and excellent stability against moisture and air.³⁹⁻⁴³ Nevertheless, although the advances are significant, most suffer

from long reaction time^{39,40} and the need for toxic co-solvent.⁴¹⁻⁴³ Therefore, developing stable, efficient and solventless catalytic system for the synthesis of cyclic carbonate is still highly required. Herein, we reported the synthesis and characterization of a series of metal complexes bearing 2-(imidazol-2-yl)phenol ligands, which were proven to be efficient and recyclable catalysts for the reaction of various epoxides with CO₂ to selectively yield cyclic carbonates under mild conditions without any organic solvents. The catalytic performance has been systematically investigated, and the optimization of the catalytic system to produce cyclic carbonates with maximal yields was performed. The recyclability of the catalysts was also been detected. Furthermore, a proposed mechanism was given. To the best of our knowledge, the Pb(II) chelate complex was firstly used to catalyze the coupling reaction of epoxides with carbon dioxide in good catalytic activity and high selectivity.

2. Experimental section

2.1. Chemicals and analytical methods

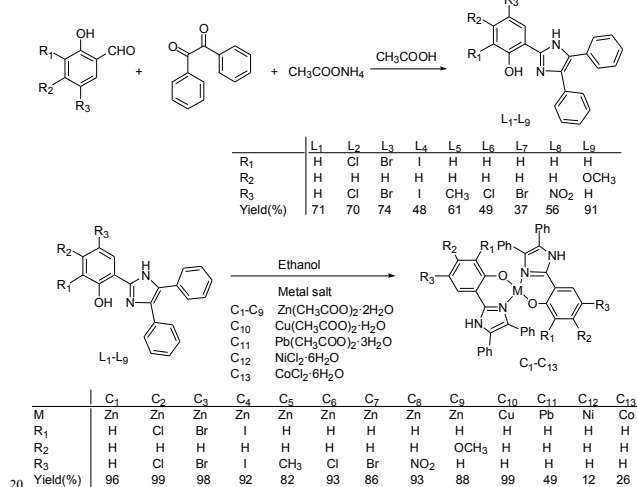
The detailed information of the materials used in present work is listed in Table S1 (see supporting information). The epoxides were distilled from CaH₂.

NMR spectra were recorded on a Bruker A1-400 MHz instrument using TMS as an internal standard. IR spectra were recorded on a Perkin-Elmer 2000 FT-IR spectrometer. Elemental analysis was conducted on a PE 2400 series II CHNS/O elemental analyzer. Melting point was obtained from X-4-type digital micro-melting point apparatus. X-ray diffraction studies

were performed on a Bruker-APEX diffractometer equipped with a CCD area detector, MoK α -radiation ($\lambda = 0.71073 \text{ \AA}$), and a graphite monochromator. Elemental analyses were performed on a Flash EA 1112 microanalyzer. IR spectra were recorded on a Nicolet 6700 FT-IR spectrometer as KBr discs in the range of 4000–600 cm^{-1} .

2.2. Synthesis of ligands L₁–L₉

The synthesis of ligands L₁–L₉ followed the general procedure shown in Scheme 1.⁴⁴ A mixture of salicylaldehyde or corresponding salicylaldehyde derivatives (9.51 mmol), benzil (9.51 mmol), and ammonium acetate (20 equivalent) were refluxed for 2 h in glacial acetic acid (30 mL) under N₂ to form a precipitate. An excess of de-ionised water was added to complete the precipitation. The crude product was collected by filtration, washed with water, and dried by suction. The resulting solid was dissolved in CH₂Cl₂ and dried over MgSO₄. The solution was filtered and the solvent was evaporated from the filtrate to produce a powder. After recrystallization from CH₂Cl₂–pentane, a crystalline solid was obtained.



Scheme 1 Synthesis of ligands L₁–L₉ and complexes C₁–C₁₃. The molecular structures of ligands are only different by substituents.

L₁ (2-(4,5-diphenyl-1H-imidazol-2-yl)phenol): 71% yield. Mp. 202 – 204 °C. Selected IR peaks (KBr, cm^{-1}): ν 3208, 3058, 1598, 1539, 1135, 1074, 695. ¹H NMR (400 MHz, DMSO) δ 13.04 (s, 1H), 12.96 (s, 1H), 8.05 (d, J = 7.6 Hz, 1H), 7.59 – 7.37 (m, 7H), 7.37 – 7.19 (m, 4H), 6.97 (m, 2H). ¹³C NMR (101 MHz, DMSO) δ 157.18, 146.33, 134.64, 130.76, 128.98, 128.80, 127.78, 127.54, 127.27, 119.33, 117.30, 113.36. Anal. Calcd for C₂₁H₁₆N₂O: C, 80.77; H, 5.13; N, 8.97%. Found: C, 81.70; H, 5.15; N, 8.95%.

L₂ (2,4-dichloro-6-(4,5-diphenyl-1H-imidazol-2-yl)phenol): 70% yield. Mp. 209 – 210 °C. Selected IR peaks (KBr, cm^{-1}): ν 3315, 3063, 1463, 1373, 1262, 1079, 696. ¹H NMR (400 MHz, DMSO) δ 8.18 (d, J = 2.5 Hz, 2H), 7.56 (m, 8H), 7.44 (s, 4H). ¹³C NMR (101 MHz, DMSO) δ 156.13, 146.57, 134.24, 131.37, 129.20, 129.11, 127.95, 127.88, 127.31, 125.63, 125.45, 118.29. Anal. Calcd for C₂₁H₁₄N₂OCl₂: C, 66.14; H, 3.67; N, 7.35%. Found: C, 66.17; H, 3.67; N, 7.34%.

L₃ (2,4-dibromo-6-(4,5-diphenyl-1H-imidazol-2-yl)phenol): 74% yield. Mp. 193 – 195 °C. Selected IR peaks (KBr, cm^{-1}): ν

3321, 3069, 1450, 1367, 1259, 1077, 697. ¹H NMR (400 MHz, DMSO) δ 8.34 (d, J = 2.3 Hz, 1H), 7.79 (d, J = 2.3 Hz, 1H), 7.54 (d, J = 7.0 Hz, 5H), 7.44 (s, 7H). ¹³C NMR (101 MHz, DMSO) δ 155.88, 146.49, 137.37, 134.63, 134.28, 129.97, 129.91, 128.12, 127.70, 122.95, 118.37, 116.64. Anal. Calcd for C₂₁H₁₄N₂OBr₂: C, 53.62; H, 2.98; N, 5.96%. Found: C, 53.65; H, 3.01; N, 5.97%.

L₄ (2,4-diiodo-6-(4,5-diphenyl-1H-imidazol-2-yl)phenol): 48% yield. Mp. 203 – 205 °C. Selected IR peaks (KBr, cm^{-1}): ν 3331, 3064, 1443, 1378, 1257, 1001, 697. ¹H NMR (400 MHz, DMSO) δ 8.45 (d, J = 2.0 Hz, 1H), 8.02 (d, J = 2.0 Hz, 1H), 7.54 (d, J = 7.1 Hz, 5H), 7.46 – 7.41 (m, 7H). ¹³C NMR (101 MHz, DMSO) δ 163.91, 147.89, 145.66, 137.49, 133.28, 129.37, 129.15, 128.73, 127.38, 121.57, 99.99, 99.84. Anal. Calcd for C₂₁H₁₄N₂OI₂: C, 44.68; H, 2.48; N, 4.96%. Found: C, 44.64; H, 2.50; N, 4.94%.

L₅ (4-methyl-2-(4,5-diphenyl-1H-imidazol-2-yl)phenol): 61% yield. Mp. 190 – 192 °C. Selected IR peaks (KBr, cm^{-1}): ν 3280, 3035, 1505, 1378, 1249, 1073, 695. ¹H NMR (400 MHz, DMSO) δ 12.97 (s, 1H), 12.67 (s, 1H), 7.89 (d, J = 1.4 Hz, 1H), 7.58 – 7.23 (m, 10H), 7.09 (m, 1H), 6.88 (d, J = 8.3 Hz, 1H), 2.30 (s, 3H). ¹³C NMR (101 MHz, DMSO) δ 155.06, 146.45, 134.70, 131.17, 130.79, 129.17, 128.95, 128.70, 127.81, 125.52, 117.07, 112.98, 20.69. Anal. Calcd for C₂₂H₁₈N₂O: C, 80.98; H, 5.52; N, 8.59%. Found: C, 80.95; H, 5.49; N, 8.58%.

L₆ (4-chloro-2-(4,5-diphenyl-1H-imidazol-2-yl)phenol): 49% yield. Mp. 198 – 200 °C. Selected IR peaks (KBr, cm^{-1}): ν 3224, 2370, 1489, 1374, 1254, 1077, 696. ¹H NMR (400 MHz, DMSO) δ 13.14 (s, 1H), 13.05 (s, 1H), 8.18 (d, J = 2.6 Hz, 1H), 7.59 – 7.43 (m, 7H), 7.33 (m, 4H), 7.02 (d, J = 8.8 Hz, 1H). ¹³C NMR (101 MHz, DMSO) δ 153.14, 147.07, 133.61, 130.25, 129.71, 129.53, 128.96, 128.83, 127.75, 127.40, 120.11, 117.93. Anal. Calcd for C₂₁H₁₅N₂OCl: C, 72.73; H, 4.33; N, 8.08%. Found: C, 72.77; H, 4.35; N, 8.08%.

L₇ (4-bromo-2-(4,5-diphenyl-1H-imidazol-2-yl)phenol): 37% yield. Mp. 181 – 183 °C. Selected IR peaks (KBr, cm^{-1}): ν 3207, 2370, 1485, 1369, 1253, 1075, 696. ¹H NMR (400 MHz, DMSO) δ 13.14 (s, 1H), 13.08 (s, 1H), 8.31 (d, J = 2.4 Hz, 1H), 7.53 (s, 5H), 7.46 – 7.34 (m, 5H), 6.97 (d, J = 8.8 Hz, 2H). ¹³C NMR (101 MHz, DMSO) δ 154.28, 147.95, 134.77, 133.82, 133.34, 129.61, 129.07, 128.93, 127.81, 120.89, 119.02, 116.28. Anal. Calcd for C₂₁H₁₅N₂OBr: C, 64.85; H, 3.84; N, 7.16%. Found: C, 64.85; H, 3.85; N, 7.19%.

L₈ (4-nitro-2-(4,5-diphenyl-1H-imidazol-2-yl)phenol): 56% yield. Mp. 250 – 252 °C. Selected IR peaks (KBr, cm^{-1}): ν 3295, 2367, 1486, 1334, 1296, 1130, 696. ¹H NMR (400 MHz, DMSO) δ 14.12 – 13.82 (m, 2H), 9.16 (d, J = 2.7 Hz, 1H), 8.18 (m, 1H), 7.61 – 7.49 (m, 4H), 7.42 (m, 6H), 7.19 (d, J = 9.1 Hz, 1H). ¹³C NMR (101 MHz, DMSO) δ 158.32, 144.51, 138.79, 130.03, 129.55, 129.31, 128.47, 128.22, 124.92, 123.76, 118.23, 99.99. Anal. Calcd for C₂₁H₁₅N₃O₂: C, 73.90; H, 4.40; N, 12.32%. Found: C, 73.86; H, 4.42; N, 12.34%.

L₉ (5-methoxy-2-(4,5-diphenyl-1H-imidazol-2-yl)phenol): 91% yield. Mp. 220 – 221 °C. Selected IR peaks (KBr, cm^{-1}): ν 3225, 3061, 2939, 1604, 1445, 1268, 1201, 1075, 696. ¹H NMR (400 MHz, DMSO) δ 13.11 (s, 1H), 12.84 (s, 1H), 7.95 (d, J = 8.4 Hz, 1H), 7.48 (m, 7H), 7.31 (m, 3H), 6.60 – 6.52 (m, 2H), 3.79 (s, 3H). ¹³C NMR (101 MHz, DMSO) δ 162.03, 156.19, 146.97, 132.92, 129.37, 129.13, 128.91, 128.32, 127.46, 110.98, 108.47,

102.95, 54.73. Anal. Calcd for $C_{22}H_{18}N_2O_2$: C, 77.19; H, 5.26; N, 8.19%. Found: C, 77.15; H, 5.30; N, 8.16%.

2.3. Synthesis of complexes C_1 – C_{13}

The synthesis of complexes C_1 – C_{13} followed the general procedure shown in Scheme 1.⁴⁴ Ligands L_1 – L_9 (12.50 mmol) and corresponding metal salts (6.30 mmol) were dissolved in 50 mL of ethanol and refluxed at 70 °C for 3 h. The resulting precipitate was filtered, washed with a few milliliters of ethanol, and dried to obtain complexes C_1 – C_{13} .

C_1 (bis(2-(4,5-diphenyl-1H-imidazol-2-yl)phenoxy)zinc): 96% yield. Mp. 336 – 338 °C. Selected IR peaks (KBr, cm^{-1}): ν 3414, 3057, 1604, 1534, 1481, 1312, 1260, 697. 1H NMR (400 MHz, DMSO) δ 12.62 (s, 2H), 7.76 (d, J = 6.3 Hz, 2H), 7.32 (m, 10H), 7.16 (t, J = 7.8 Hz, 2H), 7.12 – 6.92 (m, 6H), 6.84 (t, J = 7.7 Hz, 4H), 6.75 (d, J = 8.3 Hz, 2H), 6.55 (t, J = 6.8 Hz, 2H). ^{13}C NMR (101 MHz, DMSO) δ 156.10, 136.93, 133.24, 130.79, 129.76, 129.48, 128.92, 128.74, 127.68, 121.86, 119.05, 116.65, 58.23. Anal. Calcd for $C_{42}H_{30}N_4O_2Zn \cdot COOCH_3$: C, 70.78; H, 4.42; N, 7.51%. Found: C, 70.75; H, 4.43; N, 7.54%.

C_2 (bis(2,4-dichloro-6-(4,5-diphenyl-1H-imidazol-2-yl)phenoxy)zinc): 99% yield. Mp. 340 – 342 °C. Selected IR peaks (KBr, cm^{-1}): ν 3414, 3180, 1599, 1529, 1467, 1392, 1247, 698. 1H NMR (400 MHz, DMSO) δ 12.98 (s, 2H), 10.29 (d, 4H), 7.29 – 7.89 (m, 14H), 6.86 – 7.06 (m, 6H). ^{13}C NMR (101 MHz, DMSO) δ 154.63, 135.86, 133.81, 131.02, 129.74, 129.29, 128.85, 128.82, 127.39, 126.83, 126.21, 121.43, 53.97. Anal. Calcd for $C_{42}H_{26}N_4O_2Cl_4Zn \cdot COOCH_3$: C, 59.73; H, 3.28; N, 6.33%. Found: C, 59.71; H, 3.30; N, 6.34%.

C_3 (bis(2,4-dibromo-6-(4,5-diphenyl-1H-imidazol-2-yl)phenoxy)zinc): 98% yield. Mp. 335 – 337 °C. Selected IR peaks (KBr, cm^{-1}): ν 3412, 3063, 1596, 1525, 1462, 1389, 1249, 699. 1H NMR (400 MHz, DMSO) δ 13.00 (s, 2H), 8.03 (s, 2H), 7.67 (s, 2H), 7.34 (d, J = 10.4 Hz, 10H), 7.02 (d, J = 7.0 Hz, 6H), 6.89 (s, 4H). ^{13}C NMR (101 MHz, DMSO) δ 158.25, 136.14, 135.98, 133.72, 133.31, 129.63, 129.28, 128.90, 127.48, 122.79, 118.37, 116.62, 58.23. Anal. Calcd for $C_{42}H_{26}N_4O_2Br_4Zn$: C, 50.25; H, 2.59; N, 5.58%. Found: C, 50.29; H, 2.54; N, 5.59%.

C_4 (bis(2,4-diiodo-6-(4,5-diphenyl-1H-imidazol-2-yl)phenoxy)zinc): 92% yield. Mp. 280 – 281 °C. Selected IR peaks (KBr, cm^{-1}): ν 3418, 1594, 1505, 1455, 1390, 1251, 696. 1H NMR (400 MHz, DMSO) δ 12.97 (s, 2H), 8.12 (s, 2H), 7.93 (s, 2H), 7.34 (d, J = 6.2 Hz, 10H), 7.01 (d, J = 6.7 Hz, 6H), 6.87 (s, 4H). ^{13}C NMR (101 MHz, DMSO) δ 163.23, 145.86, 136.94, 137.63, 133.28, 129.49, 129.42, 128.84, 127.63, 127.49, 89.81, 89.58, 60.16. Anal. Calcd for $C_{42}H_{26}N_4O_2I_4Zn \cdot COOCH_3$: C, 42.24; H, 2.32; N, 4.48%. Found: C, 42.25; H, 2.34; N, 4.50%.

C_5 (bis(4-methyl-2-(4,5-diphenyl-1H-imidazol-2-yl)phenoxy)zinc): 82% yield. Mp. 352 – 354 °C. Selected IR peaks (KBr, cm^{-1}): ν 3052, 2920, 1598, 1494, 1444, 1305, 1242, 696. 1H NMR (400 MHz, DMSO) δ 12.57 (s, 2H), 7.98 – 7.82 (m, 2H), 7.60 (s, 2H), 7.30 (m, 12H), 7.00 (m, 6H), 6.93 – 6.74 (m, 4H), 2.27 (d, J = 20.4 Hz, 4H), 1.84 (s, 2H). ^{13}C NMR (101 MHz, DMSO) δ 152.91, 135.22, 133.34, 131.96, 131.63, 130.12, 129.62, 129.43, 128.69, 127.67, 118.74, 116.83, 56.29, 25.31. Anal. Calcd for $C_{44}H_{34}N_4O_2Zn$: C, 73.85; H, 4.76; N, 7.83%. Found: C, 73.81; H, 4.77; N, 7.86%.

C_6 (bis(4-chloro-2-(4,5-diphenyl-1H-imidazol-2-yl)phenoxy)zinc): 93% yield. Mp. 362 – 364 °C. Selected IR

peaks (KBr, cm^{-1}): ν 3054, 1598, 1478, 1379, 1306, 1242, 696. 1H NMR (400 MHz, DMSO) δ 12.77 (s, 2H), 7.87 (d, J = 2.9 Hz, 2H), 7.55 – 7.21 (m, 10H), 7.20 – 6.97 (m, 8H), 6.88 (t, J = 7.9 Hz, 4H), 6.74 (d, J = 9.0 Hz, 2H). ^{13}C NMR (101 MHz, DMSO) δ 152.37, 135.72, 132.04, 130.26, 129.78, 129.53, 128.98, 128.64, 128.30, 128.16, 120.31, 118.89, 56.49. Anal. Calcd for $C_{42}H_{28}N_4O_2Cl_2Zn$: C, 66.67; H, 3.70; N, 7.41%. Found: C, 66.70; H, 3.72; N, 7.45%.

C_7 (bis(4-bromo-2-(4,5-diphenyl-1H-imidazol-2-yl)phenoxy)zinc): 86% yield. Mp. 383 – 385 °C. Selected IR peaks (KBr, cm^{-1}): ν 3054, 2370, 1598, 1478, 1376, 1306, 1242, 697. 1H NMR (400 MHz, DMSO) δ 12.78 (s, 2H), 7.98 (s, 2H), 7.59 – 7.16 (m, 12H), 7.04 (m, 6H), 6.89 (t, J = 7.7 Hz, 4H), 6.70 (d, J = 9.1 Hz, 2H). ^{13}C NMR (101 MHz, DMSO) δ 154.93, 137.63, 134.68, 133.27, 133.19, 128.99, 128.67, 128.31, 128.17, 120.97, 118.54, 104.20, 55.94. Anal. Calcd for $C_{42}H_{28}N_4O_2Br_2Zn$: C, 59.64; H, 3.31; N, 6.63%. Found: C, 59.61; H, 3.34; N, 6.62%.

C_8 (bis(4-nitro-2-(4,5-diphenyl-1H-imidazol-2-yl)phenoxy)zinc): 93% yield. Mp. 399 – 401 °C. Selected IR peaks (KBr, cm^{-1}): ν 3245, 1604, 1563, 1484, 1306, 1133, 693. 1H NMR (400 MHz, DMSO) δ 13.35 (s, 2H), 8.94 (s, 2H), 8.07 (s, 2H), 7.35 (d, J = 18.8 Hz, 10H), 6.98 (d, J = 20.9 Hz, 6H), 6.93 (d, 4H), 6.84 – 6.79 (m, 2H). ^{13}C NMR (101 MHz, DMSO) δ 162.04, 141.77, 136.76, 133.12, 129.73, 129.34, 128.74, 127.89, 123.86, 122.75, 119.84, 117.43, 59.88. Anal. Calcd for $C_{42}H_{28}N_6O_6Zn$: C, 64.86; H, 3.60; N, 10.81%. Found: C, 64.84; H, 3.61; N, 10.86%.

C_9 (bis(5-methoxy-2-(4,5-diphenyl-1H-imidazol-2-yl)phenoxy)zinc): 88% yield. Mp. 356 – 358 °C. Selected IR peaks (KBr, cm^{-1}): ν 3226, 3053, 1606, 1546, 1447, 1322, 1155, 696. 1H NMR (400 MHz, DMSO) δ 12.43 (s, 2H), 7.69 (d, J = 8.8 Hz, 2H), 7.31 (m, 10H), 7.04 (m, 6H), 6.88 (t, J = 7.6 Hz, 4H), 6.27 (d, J = 2.7 Hz, 2H), 6.23 – 6.15 (m, 2H), 3.75 (s, 6H). ^{13}C NMR (101 MHz, DMSO) δ 168.40, 162.47, 148.89, 133.58, 129.69, 128.95, 128.69, 128.32, 128.08, 127.49, 126.23, 106.74, 102.30, 55.13. Anal. Calcd for $C_{44}H_{34}N_4O_4Zn$: C, 70.68; H, 4.55; N, 7.50%. Found: C, 70.66; H, 4.54; N, 7.51%.

C_{10} (bis(2-(4,5-diphenyl-1H-imidazol-2-yl)phenoxy)copper): 99% yield. Mp. 226 – 228 °C. Selected IR peaks (KBr, cm^{-1}): ν 3410, 3057, 1604, 1540, 1480, 1315, 1142, 696. A resolvable NMR spectrum could not be measured owing to paramagnetism.⁴⁵ Anal. Calcd for $C_{42}H_{30}N_4O_2Cu \cdot CH_3CH_2OH$: C, 72.18; H, 4.92; N, 7.66%. Found: C, 72.17; H, 4.89; N, 7.68%.

C_{11} (bis(2-(4,5-diphenyl-1H-imidazol-2-yl)phenoxy)lead): 49% yield. Mp. 234 – 236 °C. Selected IR peaks (KBr, cm^{-1}): ν 3418, 3060, 1600, 1528, 1482, 1245, 1139, 699. A resolvable NMR spectrum could not be measured owing to paramagnetism.⁴⁶ Anal. Calcd for $C_{21}H_{15}ON_2Pb \cdot 2COOCH_3$: C, 47.17; H, 3.30; N, 4.40%. Found: C, 47.18; H, 3.32; N, 4.41%.

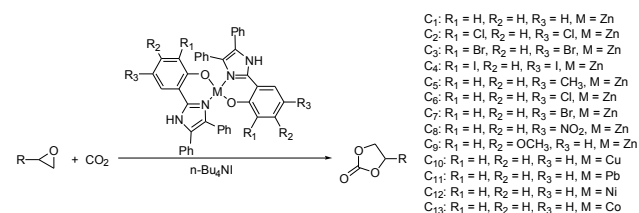
C_{12} (bis(2-(4,5-diphenyl-1H-imidazol-2-yl)phenoxy)nickel): 12% yield (0.03 g). Mp. 360 – 363 °C. Selected IR peaks (KBr, cm^{-1}): ν 3424, 3062, 1604, 1533, 1483, 1253, 1142, 696. A resolvable NMR spectrum could not be measured owing to paramagnetism.⁴⁷ Anal. Calcd for $C_{42}H_{30}N_4O_2Ni \cdot Cl \cdot CH_3CH_2OH$: C, 69.27; H, 4.72; N, 7.35%. Found: C, 69.27; H, 4.70; N, 7.37%.

C_{13} (bis(2-(4,5-diphenyl-1H-imidazol-2-yl)phenoxy)cobalt): 26% yield. Mp. 362 – 365 °C. Selected IR peaks (KBr, cm^{-1}): ν 3412, 3060, 1604, 1533, 1482, 1243, 1143, 696. A resolvable NMR spectrum could not be measured owing to

paramagnetism.⁴⁸ Anal. Calcd for C₄₂H₃₀N₄O₂Co·Cl·CH₃CH₂OH: C, 69.25; H, 4.72; N, 7.34%. Found: C, 69.23; H, 4.73; N, 7.31%.

2.4. General procedure for the coupling reaction of epoxides and CO₂

A typical procedure for the coupling reaction of CO₂ and epoxide was as following (Scheme 2): A stainless steel autoclave (250 mL) was linked to CO₂ cylinders. A prescribed amount of epoxide was added with a hypodermic syringe. The catalysts were successively charged into the reactor without using any additional solvent. The reactor vessel was sealed and immersed into a oil bath at the desired temperature under stirring. Then, the CO₂ was pressurized into the reactor to the given pressure and the reaction started. After the given time, the reaction was stopped and the vessel was then cooled quickly by placing in an ice water and the pressure was released slowly. The result mixture was transferred to a 50 ml round bottom flask. The unreacted propylene oxide was removed in vacuo. The yield was calculated either by taking the weight of the result product or by comparing the ratio of the product to substrate peak areas obtained by ¹H NMR analysis. The selectivity of cyclic carbonate was determined by GC/MS (HP6890/5973). For all the experiments with different catalysts, no byproduct was detected.



Scheme 2 Cycloaddition of PO and CO₂ to give PC and the metal catalysts C₁-C₁₃ used in this study.

3. Results and discussion

3.1. X-ray crystallographic studies

The compounds C₁ and C₅ could be crystallized by slow evaporation of concentrate methanol solution. The formation of the complexes C₁ and C₅ was confirmed using single crystal X-ray crystallography (Fig. 1), and their crystallographic data, selected bond lengths and angles were reported in Table 1 and Table 2, respectively. The X-ray crystallographic characterizations have shown that each complex contains a zinc centre with a distorted tetrahedral N₂O₂-coordination sphere. The zinc centre of both complexes C₁ and C₅ possessed a cis-arrangement of the phenol O-donor atoms; i.e. the two 4,5-diphenyl imidazole units were accommodated on the same side of the complexes. The two ligands of each complex are related by a C₂-axis, but the two ligands are structurally inequivalent. Though the geometry at each zinc centre could be best described as a distorted tetrahedron in which two chelating ligands were placed in a similar disposition about the zinc centre, slight differences of the bond length and dihedral angle still occurred (Table 2), which indicated that in each complex, the orientation of the two ligands accommodated the normal geometrical preference of the zinc centre.⁴⁹⁻⁵²

3.2. Catalytic performances of C₁ with various additives

The activity of various additives was tested using the reaction of PO and CO₂ to produce PC, and the results are summarized in Table 3. Both the catalyst C₁ and the co-catalyst n-Bu₄NI could catalyze the cycloaddition alone, but the yields of PC were very low (entries 1, 2). As expected, the addition of moderate amounts of co-catalyst could greatly improve the yield of PC, TON value and TOF value (entry 3 vs 1, 2), especially for the quaternary ammonium salts. As for the quaternary ammonium salts (n-Bu₄NI, n-Bu₄NBr, and n-Bu₄NCl), the effect of halide anions I⁻, Br⁻, and Cl⁻ on the catalytic activity (entries 3-5) showed that the catalytic activity improved with the increase of leaving ability (I⁻ > Br⁻ > Cl⁻).⁵³ Under the same condition, however, the activity decreased with other co-catalysts like Et₄NBr, PPh₃, DMAP and KI (entries 6-9). Therefore, n-Bu₄NI was selected as the co-catalyst to study the effect of reaction conditions on the coupling reaction in the presence of catalyst C₁.

Table 1 Crystallographic data for complexes C₁ and C₅

Identification code	C ₁ ·3CH ₃ OH	C ₅ ·2CH ₃ OH
Empirical formula	C ₄₂ H ₃₀ N ₄ O ₂ Zn·C ₃ H ₇ O ₃	C ₄₄ H ₃₄ N ₄ O ₂ Zn·C ₂ H ₆ O ₂
Formula weight (g mol ⁻¹)	784.20	780.21
Crystal size (mm ³)	0.12 × 0.10 × 0.10	0.12 × 0.10 × 0.10
Crystal system	Triclinic	Monoclinic
Space group	P 1	C2/c
<i>Unit cell dimensions</i>		
a (Å)	12.366(3)	28.552(3)
b (Å)	12.634(3)	13.6389(12)
c (Å)	14.695(4)	19.5849(18)
α (°)	67.273(3)	90
β (°)	67.681(4)	94.9510(10)
γ (°)	75.098(4)	90
Volume (Å ³)	1942.4(8)	7598.3(12)
Z	2	8
D _{calc} (g/cm ³)	1.341	1.364
σ (mm ⁻¹)	0.684	0.697
Collected refl.	36849	7972
Independent refl. (R _{int})	7490(0.0504)	10991(0.0787)
Parameters	502	502
R ₁ [> 2σ(I)]	0.0779	0.0363
wR ₂ (all data)	0.2323	0.1130
GOF	1.080	1.101

Table 2 Selected bond distances (Å) and angles (°) for compounds C₁ and C₅

	C ₁ ·3CH ₃ OH	C ₅ ·2CH ₃ OH
<i>Bond distances (Å)</i>		
Zn(1)-O(2)	1.944(2)	1.9375(9)
Zn(1)-O(1)	1.940(2)	1.9336(9)
Zn(1)-N(1)	1.972(3)	1.9925(11)
Zn(1)-N(3)	1.979(3)	1.9801(11)
<i>Bond angles (°)</i>		
O(2)-Zn(1)-O(1)	110.21(11)	116.94(4)
O(2)-Zn(1)-N(1)	121.40(11)	113.53(4)
O(1)-Zn(1)-N(1)	96.15(11)	96.06(4)
O(2)-Zn(1)-N(3)	94.63(10)	94.59(4)
O(1)-Zn(1)-N(3)	110.17(11)	115.46(4)
N(1)-Zn(1)-N(3)	124.40(11)	121.92(4)

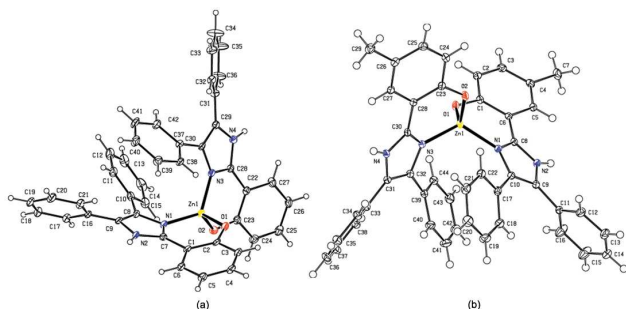


Fig. 1 ORTEP representations of the molecular structures of (a) complex C_1 and (b) complex C_5 . Structural differences are caused by steric effects of substituent on the imidazole ring.

Table 3 Coupling of CO_2 and PO catalyzed by various components^a

Entry	Catalyst	Yield (%) ^b	TON ^c	TOF (h ⁻¹) ^d
1	C_1	3.5	35.0	7.0
2	n-Bu ₄ NI	21.7	254.0	50.8
3	C_1 /n-Bu ₄ NBr	91.4	914.0	182.8
4	C_1 /n-Bu ₄ NCl	42.4	423.5	84.7
5	C_1 /n-Bu ₄ NI	95.8	958.0	191.6
6	C_1 /Et ₄ NBr	87.3	873.0	174.6
7	C_1 /PPh ₃	5.5	55.0	11.0
8	C_1 /DMAP	12.6	125.5	25.1
9	C_1 /KI	52.1	521.0	104.2

^a Catalyst: 0.214 mmol; co-catalyst: 0.214 mmol; PO: 15 mL, 0.214 mol; CO_2 pressure: 5 MPa; time: 5 h; temperature: 130 °C, the selectivity to products are all > 99 %. ^b Isolated yields. ^c Turnover number for PC calculated as moles of PC produced per mole of catalyst. ^d Turnover frequency for PC calculated as mole of PC produced per mole of catalyst per hour.

3.3. The effect of reaction pressure

Generally, a significant disadvantage associated with CO_2 as reagent or reaction medium in organic synthesis is the potential dangers operated at high pressures.²⁴ Thus, the effect of CO_2 pressure on the catalytic activity was studied at 130 °C in pressure range of 1-7 MPa, and the results are shown in Fig. 2. PC yield increased dramatically with increasing pressure in the range of 1-2 MPa, then remained almost constant with further increase in pressure. The further CO_2 pressure increase beyond 2 MPa apparently favored a slightly increased PC formation, but the rise is unnecessary. This may be attributed to the phase behaviour of CO_2 -PO system which resulted in the effect of pressure on the concentrations of CO_2 and PO.⁵⁴ There were three phases in the reaction system including the top CO_2 -rich gas phase, catalyst-rich solid phase and the bottom PO-rich liquid phase. The reaction mostly took place in the PO-catalyst interface. The initial increase of CO_2 pressure (0-2 MPa) led to the increased concentration of CO_2 in the liquid phase, which is why the PC yield was raised significantly. Nevertheless, the PC yield no longer increased with the CO_2 pressure beyond 2 MPa up to 7 MPa. This may be due to the higher pressure extracted a certain amount of PO into the gas phase, and caused the decline of PO concentration in the vicinity of the catalyst in the liquid phase.⁵⁵ Besides, the instrument which is operated under high pressure condition is too expensive to afford in industry application. Therefore, 2 MPa was chosen as the optimal reaction pressure in the following catalytic reaction of CO_2 and PO to PC.

3.4. The effect of reaction time

The PC yield versus reaction time was shown in Fig. 3. The PC synthesis from PO and CO_2 proceeded rapidly, and nearly 80% PC yield was obtained within the first 3 h at 130 °C. The PC yield experienced a continuing growth within 5 h, and then gradually

decreased. It is noted that a further increase in the reaction time led to a slight decrease in PC yield. This may be due to that the interaction between catalysts and reactant was obstructed by the formed PC.⁵⁶ The growing viscosity of the reaction system was also another negative factor for the activation of CO_2 at longer reaction time. The selectivity of PC stayed above 99% throughout. So, a reaction time of 5 h was required for further research.

3.5. The effect of reaction temperature

The effect of the temperature on the cycloaddition reaction catalyzed by C_1 in the presence of n-Bu₄NI in the temperature range of 50-130 °C was shown in Fig. 4. The figure illustrated that the activity of the catalyst was strongly affected by reaction temperature.⁵⁷ The yield of PC increased with increasing temperature, and reached 90.3% at 110 °C, then the PC yield only slightly increased with further increase of temperature, indicating that 110 °C was the optimal temperature. It is also interesting to note that no by-product polyether was detected even at very low temperature, which indicated that the catalyst used in this work had a good selectivity for the production of PC.⁵⁸

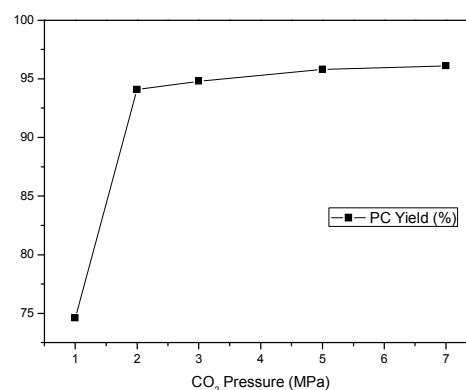


Fig. 2 Effect of CO_2 pressure on PC yield. Reaction conditions: 0.214 mmol C_1 , 0.214 mmol n-Bu₄NI, 0.214 mol PO, reaction temperature 130 °C, reaction time 5 h, the selectivity to products are all > 99 %.

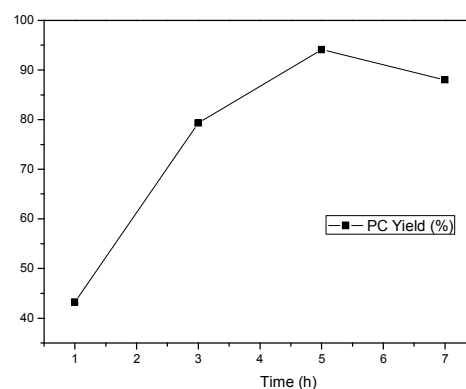


Fig. 3 Effect of reaction time on PC yield. Reaction conditions: 0.214 mmol C_1 , 0.214 mmol n-Bu₄NI, 0.214 mol PO, reaction temperature 130 °C, CO_2 pressure 2 MPa, the selectivity to products are all > 99 %.

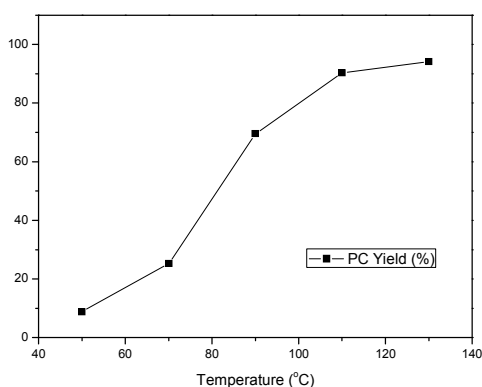


Fig. 4 Effect of reaction temperature on PC yield. Reaction conditions: 0.214 mmol C₁, 0.214 mmol n-Bu₄NI, 0.214 mol PO, reaction time 5 h, CO₂ pressure 2 MPa, the selectivity to products are all > 99 %.

3.6. Effect of substitution on the aromatic rings of Complexes

The substitution on the aromatic rings of salicylaldehyde probably causes geometrical distortion of space structure, and thus, may affect properties of catalyst. So, the effect of substitution on the aromatic rings of complexes was investigated. The experimental results in Table 4 showed that although this series of catalysts had good catalytic performance under optimal conditions (110 °C, 5 h, 2 MPa), the catalytic activity of these catalysts exhibited some difference for different substitutions. Under the same conditions, catalytic activities of 3,5-substituted complexes were in the following order: C₄ (-I) (95.9%) > C₃ (-Br) (94.2%) > C₂ (-Cl) (94.0%) > C₁ (-H) (90.3%), which indicated that the electron-withdrawing effect played a key role in the decrease of catalytic property of these zinc complexes.^{59,60} For the 5-substituted Zn complexes, the order was: C₇ (-Br) (99.7%) > C₆ (-Cl) (94.6%) > C₈ (-NO₂) (94.1%) > C₅ (-CH₃) (89.3%), while the order of electron-withdrawing effect was: -NO₂ > -Cl > -Br > -CH₃. The exception of C₅ (-CH₃) might be attributed to the steric hindrance effect of methyl, which was not benefit for the insertion of propylene oxide into the metal centre.⁶¹ Ko and co-workers had reported homologous zinc catalysts bearing iminebenzotriazole phenoxide ligands,⁶² which were active catalyst (TOF: 33.3 h⁻¹) for the cycloaddition of CO₂ with propylene oxide in the presence of n-Bu₄NBr to give propylene carbonate (PC) under mild conditions (table 4, entry 10). Both Ko's and present works proved that zinc complexes with phenoxide ligands possessed excellent catalytic performance for the coupling reaction of CO₂ and epoxide.

Table 4 Effect of substitution on the aromatic rings on the catalytic activity^a

Entry	Catalyst	Yield (%) ^b	TON ^c	TOF (h ⁻¹) ^d
1	C ₁ /n-Bu ₄ NI	90.3	903.0	180.6
2	C ₂ /n-Bu ₄ NI	94.0	940.0	188.0
3	C ₃ /n-Bu ₄ NI	94.2	942.0	188.4
4	C ₄ /n-Bu ₄ NI	95.9	959.0	191.8
5	C ₅ /n-Bu ₄ NI	89.3	893.0	178.6
6	C ₆ /n-Bu ₄ NI	94.6	946.0	189.2
7	C ₇ /n-Bu ₄ NI	99.7	997.0	199.4
8	C ₈ /n-Bu ₄ NI	94.1	941.0	188.2
9	C ₉ /n-Bu ₄ NI	90.2	902.0	180.4
10 ^e	(^{C⁸F¹⁰} IBTP) ₂ Zn/n-Bu ₄ NI	37.0	370.0	15.4
12	C ₁₀ /n-Bu ₄ NI	56.2	562.0	112.4
13	C ₁₁ /n-Bu ₄ NI	80.1	801.0	160.2
14	C ₁₂ /n-Bu ₄ NI	81.2	812.0	162.4
15	C ₁₃ /n-Bu ₄ NI	91.1	911.0	182.2

^a Catalyst: 0.214 mmol; n-Bu₄NI: 0.214 mmol; PO: 15 mL, 0.214 mol; CO₂ pressure: 2 MPa; time: 5 h; temperature: 110 °C, the selectivity to products are all > 99 %. ^b Isolated yields. ^c Turnover number for PC calculated as moles of PC produced per mole of catalyst. ^d Turnover frequency for PC calculated as mole of PC produced per mole of catalyst per hour. ^e Ref. 62: Catalyst (mol%): 0.1, PO: 5.0 mL, 50 °C, 1.0 MPa initial CO₂ pressure, 24 h.

3.7. Effect of central metal on the activity

In order to make a systematic comparison, the catalytic properties of C₁₀ (Cu), C₁₁ (Pb), C₁₂ (Ni), and C₁₃ (Co) were also investigated (Table 4). Except Cu centre, the PC yield catalyzed by other four metal centre complexes (Zn, Pb, Ni, Co) were all > 80%, and the activity order was C₁₃ (Co) (91.1%) > C₁ (Zn) (90.3%) > C₁₂ (Ni) (81.2%) > C₁₁ (Pb) (80.1%) > C₁₀ (Cu) (56.2%), which indicated that the catalytic activity is highly dependent on the type of centre metal. It is possible that the high catalytic activities of the cobalt(II)-, zinc(II)-, nickel(II)-, lead(II)-centre complexes and the low activity of the copper(II)-centre complexes are related to the metal's different coordination ability with PO.^{63,64} It's worthily noted that most Pb or Pb(II) compounds were used as electrodes for the electrochemical reduction of CO₂.⁶⁵ The present study is the first report about the usefulness of lead catalyst for coupling reaction between CO₂ and epoxides.

3.8. Catalyst recycling

As well-known, the stability and reusability of a catalyst are two key factors for practical application in industry. Catalyst C₁ was chosen to evaluate the recyclability, and then a series of catalytic cycles for the coupling reaction of CO₂ with PO was carried out under the optimized reaction conditions (110 °C, 5 h, 2 MPa). In each cycle, the catalyst C₁ could be easily separated from the product by the addition of ethanol, subsequent filtration and then used for the next run directly. The results in Fig. 5 exhibited that the catalyst C₁ could be reusable for at least 5 times without significant loss of activity, while the selectivity of the product remained the same.

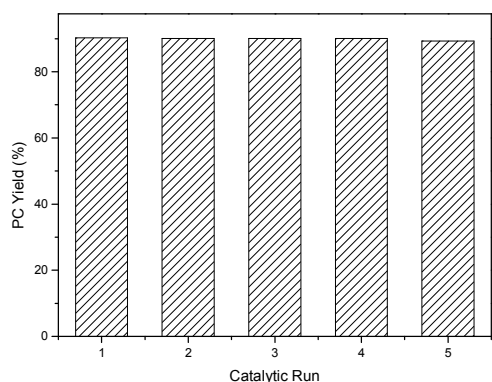


Fig. 5 Catalyst recycling with 0.214 mmol C_1 /0.214 mmol $n\text{-Bu}_4\text{NI}$ /0.214 mol PO at 110 °C, 2 MPa CO_2 , and 5 h (>99 % PC selectivity is maintained).

3.9. Applicability of substrates

The catalytical performance of $C_1/n\text{-Bu}_4\text{NI}$ for the cycloaddition of CO_2 with other epoxides were also studied at 110 °C, 5 h and 2 MPa without any organic solvent, and the results are summarized in Table 5. The catalyst was applicable to a variety of terminal epoxides to produce the corresponding cyclic carbonates with excellent yields, with the exception of isobutylene oxide (entry 5) and cyclohexene oxide (entry 6), which was probably due to their higher steric hindrance.^{66,67} This steric effect was more likely to hinder the nucleophilic attack of the epoxide rather than its coordination to the Lewis acid metal centre.^{68,69}

Table 5 Cycloaddition between CO_2 and various epoxides catalyzed by C_1 in the presence of $n\text{-Bu}_4\text{NI}$ ^a

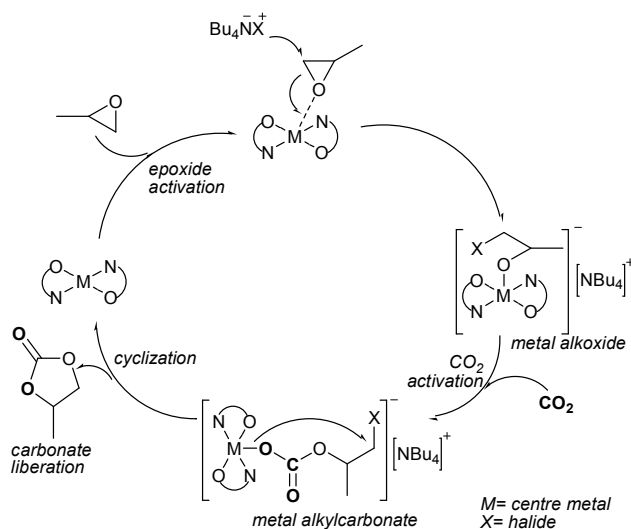
Entry	Epoxide	Product	Yield (%) ^b	TON ^c	TOF (h ⁻¹) ^d
1			98.1	981.0	196.2
2			93.8	938.0	187.6
3			93.1	931.0	186.2
4			93.4	934.0	186.8
5			19.3	193.0	38.6
6			42.6	426.0	85.2

^a C_1 : 0.214 mmol; $n\text{-Bu}_4\text{NI}$: 0.214 mmol; epoxide: 0.214 mol; CO_2 pressure: 2 MPa; time: 5 h; temperature: 110 °C, the selectivity to products are all > 99 %. ^b Isolated yields. ^c Turnover number for carbonates calculated as moles of carbonate produced per mole of catalyst. ^d Turnover frequency for carbonates calculated as mole of carbonate produced per mole of catalyst per hour.

3.10. Proposed mechanism of the coupling reaction

The metal-catalyzed coupling reaction of CO_2 and epoxides is generally thought to occur via a coordination-insertion mechanism.⁷⁰ Taking into account the diverse mechanisms found in the literature for the coupling of epoxide and CO_2 ⁷¹⁻⁷⁴ and DFT studies involving in particular zinc salphen,⁶⁹ a general mechanism can be illustrated for the $\text{M-N}_2\text{O}_2/(n\text{-Bu})_4\text{NX}$ catalytic system in Scheme 3. Considering that the reports on ionic metal salen's of the type $[\text{N}_2\text{O}_2\text{M-X}][\text{NR}_4]$ have been scarce,

a neutral $\text{M-N}_2\text{O}_2$ species as the starting point in the catalytic cycle.⁴⁰ The ligands of the catalysts comprise a N_2O_2 coordination pocket into which a wide variety of metal ions can be easily accommodated and that function as the catalytic center. Various substituents can be easily introduced in the aromatic rings to allow, for example, control over the approach of a substrate by bulky groups or variation of the Lewis acidity of the metal center through electron-withdrawing/donating groups. The insertion of appropriate substituents on the phenyl ring can also be employed to anchor the salen scaffold to a solid support, thus allowing for the preparation of heterogeneous catalysts.⁷⁵ The epoxide ring of PO was activated by $\text{M-N}_2\text{O}_2$ species, and then the epoxide ring was attacked by the anion of co-catalyst such as $n\text{-Bu}_4\text{NI}$, leading to epoxide ring-opening and formation of a metal-bound alkoxide. At the same time, CO_2 inserted into the metal-alkoxide bond to form a metal alkylcarbonate, and then the production of cyclic carbonate was formed via a backbiting pathway.⁷⁶ This mechanism indicated that the presence of a nucleophilic group, either a nucleophilic axial anion or an added co-catalyst, and a metal centre were both necessary for the reaction, that is why the PC yield was very low when catalyzed by the metal complex C_1 or co-catalyst $n\text{-Bu}_4\text{NI}$ alone (Table 4, entries 1 and 2).



Scheme 3 Proposed mechanism for cyclic carbonate formation.

Conclusions

In summary, a series of easily accessible metal complexes bearing 2-(imidazol-2-yl)phenol ligands were synthesized and characterized. Systematical investigation demonstrated that all the complexes were active and versatile catalysts for the coupling reaction of CO_2 and epoxides to selectively generate cyclic carbonate without any organic solvents. The effect of reaction conditions (time, temperature and pressure), substitution on the aromatic rings of ligands and central metal on the catalytic activity were investigated, and the optimal catalytical conditions were screened as 110 °C, 5 h, 2 MPa. The catalyst also could be reused several times with only minor loss in the catalyst activity. This catalyst system was also suitable for the production of cyclic carbonates from CO_2 and epoxides. These characteristics made them ideal catalysts in terms of potential industrial application in chemical CO_2 fixation.

Acknowledgements

We are grateful to National Natural Science Foundation of China (No. 51073175).

Abbreviations

CO₂, carbon dioxide; PO, propylene oxide; PC, propylene carbonate; MOFs, metal–organic frameworks; CaH₂, calcium hydride; TMS, trimethylsilane; CH₂Cl₂, dichloromethane; MgSO₄, magnesium sulfate anhydrous; DMSO, dimethylsulfoxide; DMAP, 4-dimethylaminopyridine; KI, potassium iodide; PPh₃, triphenylphosphine; n-Bu₄NBr, tetrabutylammonium bromide; n-Bu₄NCl, tetrabutylammonium chloride; n-Bu₄NI, tetrabutylammonium iodide.

Notes and references

^aThe State Key Laboratory of Power Transmission Equipment & System Security and New Technology, College of Chemistry and Chemical Engineering, Chongqing university, Chongqing 400044, China

^bKey Laboratory of Catalysis and Materials Science of the State Ethnic Affairs Commission & Ministry of Education, Hubei Province, Key Laboratory of Analytical Chemistry of the State Ethnic Affairs Commission, College of Chemistry and Materials Science, South-Central University for Nationalities, Wuhan, 430074, P.R. China. Tel./Fax: +86-27-67842752; Email addresses: yanghaijian@vip.sina.com

^cSchool of Chemistry and Chemical Engineering, University of Chinese Academy of Sciences, Beijing, 100049, P.R. China

Email addresses: cyguo@ucas.ac.cn

† Electronic Supplementary Information (ESI) available: [details of any supplementary information available should be included here]. See DOI: 10.1039/b000000x/

- 1 I. Omae, *Catal. Today*, 2006, **115**, 33.
- 2 T. Sakakura, J. C. Choi, H. Yasuda, *Chem. Rev.*, 2007, **107**, 2365.
- 3 A. T. Najafabadi, *Int. J. Energy Res.*, 2013, **37**, 485.
- 4 T. Sakakura, K. Kohno, *Chem. Commun.*, 2009, 1312.
- 5 J. Sebastian, S. Darbha, *RSC Adv.*, 2015, **5**, 18196.
- 6 D. J. Darensbourg, W. C. Chung, K. Wang, H. C. Zhou, *ACS Catal.*, 2014, **4**, 1511–1515.
- 7 R. J. Wei, X. H. Zhang, Y. Y. Zhang, B. Y. Du, Z. Q. Fan, G. R. Qi, *RSC Adv.*, 2014, **4**, 3188.
- 8 I. S. Metcalfe, M. North, P. J. Villuendas, *J. CO₂ Utilization*, 2013, **2**, 24.
- 9 Y. Xie, T. T. Wang, X. H. Liu, K. Zou, W. Q. Deng, *Nat. Commun.*, 2013, **4**, 1.
- 10 Z. Zhang, L. Xu, W. Feng, *RSC Adv.*, 2015, **5**, 12382.
- 11 J. A. Castro-Osma, C. Alonso-Moreno, A. Lara-Sánchez, J. Martínez, M. North, A. Otero, *Catal. Sci. Technol.*, 2014, **4**, 1674.
- 12 S. H. Li, B. Miao, W. M. Yuan, S. M. Ma, *Org. Lett.*, 2013, **15**, 977.
- 13 X. D. Tang, C. R. Qi, H. T. He, H. F. Jiang, Y. W. Ren, G. Q. Yuan, *Adv. Synth. Catal.*, 2013, **355**, 2019.
- 14 J. C. Choi, K. Shiraishi, Y. Takenaka, H. Yasuda, T. Sakakura, *Organometallics*, 2013, **32**, 3411.
- 15 Y. Chen, R. Qiu, X. Xu, C. T. Au, S. F. Yin, *RSC Adv.*, 2014, **4**, 11907.
- 16 N. M. Rajendran, A. Haleel, N. D. Reddy, *Organometallics*, 2014, **33**, 217.
- 17 T. Ema, Y. Miyazaki, S. Koyama, Y. Yano, T. Sakai, *Chem. Commun.*, 2012, **48**, 4489.
- 18 J. Meléndez, M. North, P. Villuendas, *Chem. Commun.*, 2009, 2577.
- 19 H. Y. Ju, M. D. Manju, K. H. Kim, S. W. Park, D. W. Park, *J. Ind. Eng. Chem.*, 2008, **14**, 157.
- 20 W. L. Dai, B. Jin, S. L. Luo, X. B. Luo, X. M. Tu, C. T. Au, *Catal. Sci. Technol.*, 2014, **4**, 556.
- 21 W. L. Wong, L. Y. S. Lee, K. P. Ho, Z. Y. Zhou, T. Fan, Z. Y. Lin, K. Y. Wong, *Appl. Catal. A*, 2014, **472**, 160.
- 22 A. Ion, V. Parvulescu, P. Jacobs, D. de Vos, *Appl. Catal. A*, 2009, **363**, 40.
- 23 J. Tharun, K. R. Roshan, A. C. Kathalikkattil, D. H. Kang, H. M. Ryu, D. W. Park, *RSC Adv.*, 2014, **4**, 41266.
- 24 M. Liu, B. Liu, L. Shi, F. Wang, L. Liang, J. Sun, *RSC Adv.*, 2015, **5**, 960.
- 25 J. Peng, H. J. Yang, N. Song, C. Y. Guo, *J. CO₂ Util.*, 2015, **9**, 16.
- 26 W. L. Dai, S. L. Luo, S. F. Yin, C. T. Au, *Appl. Catal. A*, 2009, **366**, 2.
- 27 M. Aresta, A. Dibenedetto, L. Gianfrate, C. Pastore, *Appl. Catal. A*, 2003, **25**, 5.
- 28 Q. W. Song, L. N. He, J. Q. Wang, H. Yasuda, T. Sakakura, *Green Chem.*, 2013, **15**, 110.
- 29 A. Siewniak, K. Jasiak, S. Baj, *Appl. Catal. A*, 2014, **482**, 266.
- 30 J. X. Chen, B. Jin, W. L. Dai, S. L. Deng, L. R. Cao, Z. J. Cao, S. L. Luo, X. B. Luo, X. M. Tu, C. T. Au, *Appl. Catal. A*, 2014, **484**, 26.
- 31 H. Li, P. S. Bhadury, B. Song, S. Yang, *RSC Adv.*, 2012, **2**, 12525.
- 32 S. D. Lee, B. M. Kim, D. W. Kim, M. I. Kim, K. R. Roshan, M. K. Kim, Y. S. Won, D. W. Park, *Appl. Catal. A*, 2014, **486**, 69.
- 33 J. Q. Wang, W. G. Cheng, J. Sun, T. Y. Shi, X. P. Zhang, S. J. Zhang, *RSC Adv.*, 2014, **4**, 2360.
- 34 D. Srinivas, P. Ratnasamy, *Micropor. Mesopor. Mater.*, 2007, **105**, 170.
- 35 R. Srivastava, D. Srinivas, P. Ratnasamy, *Appl. Catal. A*, 2005, **289**, 128.
- 36 Y. Ren, Y. Shi, J. Chen, S. Yang, C. Qi, H. Jiang, *RSC Adv.*, 2013, **3**, 2167.
- 37 H. Y. Cho, D. A. Yang, J. S. Kim, Y. Jeong, W. S. Ahn, *Catal. Today*, 2012, **185**, 35.
- 38 J. Kim, S. N. Kim, H. G. Jang, G. Seo, W. S. Ahn, *Appl. Catal. A*, 2013, **453**, 175.
- 39 M. A. Fuchs, S. Staudt, C. Altesleben, O. Walter, T. A. Zevaco, E. Dinjus, *Dalton Trans.*, 2014, **43**, 2344.
- 40 M. A. Fuchs, C. Altesleben, S. C. Staudt, O. Walter, T. A. Zevaco, E. Dinjus, *Catal. Sci. Technol.*, 2014, **4**, 1658.
- 41 A. Decortes, A. W. Kleij, *ChemCatChem*, 2011, **3**, 831.
- 42 M. Taherimehr, A. Decortes, S. M. Al-Amsyar, W. Lueangchaichaweng, C. J. Whiteoak, E. C. Escudero-Adán, A. W. Kleij, P. P. Pescarmona, *Catal. Sci. Technol.*, 2012, **2**, 2231.
- 43 A. Decortes, M. M. Belmonte, J. Benet-Buchholz, A. W. Kleij, *Chem. Commun.*, 2010, **46**, 4580.
- 44 A. O. Eseola, W. Li, R. Gao, M. Zhang, X. Hao, T. L. Liang, N. O. Obi-Egbedi, W. H. Sun, *Inorg. Chem.*, 2009, **48**, 9133.
- 45 S. López-Rayó, J. J. Lucena, *J. Agric. Food Chem.*, 2011, **59**, 13110.
- 46 V. K. Koltover, J. W. Logan, H. Heise, V. P. Bubnov, Y. I. Estrin, I. E. Kareev, V. P. Lodygina, A. Pines, *J. Phys. Chem. B*, 2004, **108**, 12450.
- 47 P. Chaudhuri, C. N. Verani, E. Bill, E. Bothe, T. Weyhermüller, K. Wieghardt, *J. Am. Chem. Soc.*, 2001, **123**, 2213.
- 48 M. J. Knight, I. C. Felli, R. Pierattelli, L. Emsley, G. Pintacuda, *Acc. Chem. Res.*, 2013, **46**, 2108.
- 49 L. Benisvy, A. J. Blake, D. Collison, E. S. Davies, C. D. Garner, E. J. L. McInnes, J. McMaster, G. Whittaker, C. Wilson, *Chem. Commun.*, 2001, 1824.
- 50 L. Benisvy, A. J. Blake, D. Collison, E. S. Davies, C. D. Garner, E. J. L. McInnes, J. McMaster, G. Whittaker, C. Wilson, *Dalton Trans.*, 2003, 1975.
- 51 L. Benisvy, E. Bill, A. J. Blake, D. Collison, E. S. Davies, C. D. Garner, C. I. Guindy, E. J. L. McInnes, G. McArdle, J. McMaster, C. Wilson, J. Wolowska, *Dalton Trans.*, 2004, 3647.
- 52 L. Benisvy, E. Bill, A. J. Blake, D. Collison, E. S. Davies, C. D. Garner, G. McArdle, E. J. L. McInnes, J. McMaster, S. H. K. Ross, C. Wilson, *Dalton Trans.*, 2006, 258.
- 53 Z. F. Yang, J. Sun, W. G. Cheng, J. Q. Wang, Q. Li, S. J. Zhang, *Catal. Commun.*, 2014, **44**, 6.
- 54 Y. Y. Zhang, S. F. Yin, S. L. Luo, C. T. Au, *Ind. Eng. Chem. Res.*, 2012, **51**, 3951.
- 55 W. L. Dai, B. Jin, S. L. Luo, X. B. Luo, X. M. Tu, C. T. Au, *J. Mol. Catal. A*, 2013, **378**, 326.

- 56 D. S. Bai, H. W. Jing, G. J. Wang, *Appl. Organometal. Chem.*, 2012, **26**, 600.
- 57 J. L. Song, B. B. Zhang, P. Zhang, J. Ma, J. L. Liu, H. L. Fan, T. Jiang, B. X. Han, *Catal. Today*, 2012, **183**, 130.
- 58 O. V. Zalomaeva, A. M. Chibiryayev, K. A. Kovalenko, O. A. Kholdeeva, B. S. Balzhinimaev, V. P. Fedin, *J. Catal.*, 2013, **298**, 179.
- 59 L. Dai, X. Li, H. Yuan, X. Li, Z. H. Li, D. Xu, F. Fei, Y. Q. Liu, J. Zhang, Z. M. Zhou, *Tetrahedron: Asymmetry*, 2011, **22**, 1379.
- 60 Y. Sun, W. S. Zhang, X. B. Hu, H. R. Li, *J. Phys. Chem. B*, 2010, **114**, 4862.
- 61 X. B. Lu, X. J. Feng, R. He, *Appl. Catal. A*, 2002, **234**, 25.
- 62 T. Y. Chen, C. Y. Li, C. Y. Tsai, C. H. Li, C. H. Chang, B. T. Ko, C. Y. Chang, C. H. Lin, H. Y. Huang, *J. Organomet. Chem.*, 2014, **754**, 16. (Table 3, entry 3)
- 63 S. H. Szczepankiewicz, C. M. Ippolito, B. P. Santora, T. J. Van de Ven, G. A. Ippolito, L. Fronckowiak, F. Wiatrowski, T. Power, M. Kozik, *Inorg. Chem.*, 1998, **37**, 4344.
- 64 H. Yasuda, L. N. He, T. Sakakura, C. Hu, *J. Catal.*, 2005, **233**, 119.
- 65 J. Qiao, Y. Liu, F. Hong, J. Zhang, *Chem. Soc. Rev.*, 2014, **43**, 631.
- 66 C. J. Whiteoak, N. Kielland, V. Laserna, E. C. Escudero-Adán, E. Martin, A. W. Kleij, *J. Am. Chem. Soc.*, 2013, **135**, 1228.
- 67 J. Tharun, G. Mathai, R. Roshan, A. C. Kathalikkattil, K. Bomi, D. W. Park, *Phys. Chem. Chem. Phys.*, 2013, **15**, 9029.
- 68 C. Martín, C. J. Whiteoak, E. Martin, B. M. Martínez, E. C. Escudero-Adán, A. W. Kleij, *Catal. Sci. Technol.*, 2014, **4**, 1615.
- 69 F. Castro-Gómez, G. Salassa, A. W. Kleij, C. Bo, *Chem. Eur. J.*, 2013, **19**, 6289.
- 70 S. Supasitmongkol, P. Styring, *Catal. Sci. Technol.*, 2014, **4**, 1622.
- 71 M. North, R. Pasqualem C. Young, *Green Chem.*, 2010, **12**, 1514.
- 72 M. R. Kember, A. Buchard, C. K. Williams, *Chem. Commun.*, 2011, **47**, 141.
- 73 M. Cokoja, C. Bruckmeier, B. Rieger, W. A. Herrmann, F. E. Kühn, *Angew. Chem., Int. Ed.*, 2011, **50**, 8510.
- 74 P. P. Pescarmonam M. Taherimehr, *Catal. Sci. Technol.*, 2012, **2**, 2169.
- 75 A. Decortes, A. M. Castilla, A. W. Kleij, *Angew. Chem., Int. Ed.* 2010, **49**, 9822.
- 76 A. C. Kathalikkattil, R. Roshan, J. Tharun, H. G. Soek, H. S. Ryu, D. W. Park, *ChemCatChem*, 2014, **6**, 284.